Engineering Solid Mechanics 9 (2021) 221-238

Contents lists available at GrowingScience

Engineering Solid Mechanics

homepage: www.GrowingScience.com/esm

Numerical simulation and constructal design applied to plates with different heights of traverse and longitudinal stiffeners

Carolina Martins Nogueira[a], Vinícius Torres Pinto[a], Luiz Alberto Oliveira Rocha[b], Elizaldo Domingues dos Santos[a] and Liércio André Isoldi[a*]

[a]Federal University of Rio Grande – FURG, Graduate Program in Ocean Engineering (PPGEO), Rio Grande, RS, Brazil
[b]University of Vale do Rio dos Sinos – UNISINOS, Graduate Program in Mechanical Engineering, São Leopoldo, RS, Brazil

A R T I C L E I N F O

Article history:
Received 20 May 2020
Accepted 30 July 2020
Available online
30 July 2020

Keywords:
Stiffened plates
Computational modeling
Constructal Design
Deflection
Stiffeners with different height

A B S T R A C T

This study applied the Constructal Design Method (CDM) associated with the Finite Element Method (FEM) through computational models to perform a geometric analysis on rectangular stiffened plates of steel subjected to a uniform transverse loading, in order to minimize its maximum and central out-of-plane deflections. Considering a non-stiffened plate as reference and maintaining the total volume of steel constant, a portion of material volume deducted from its thickness was transformed into stiffeners through the ϕ parameter, which represents the ratio between the material volume of the stiffeners and the reference plate. Adopting $\phi = 0.30$, 27 geometric arrangements of stiffened plates were established, being 9 arrangements for each 3 different stiffeners' thicknesses adopted: t_s = 6.35 mm, t_s = 12.70 mm and t_s = 25.40 mm. For each t_s value, the number of longitudinal (N_{ls}) and transverse (N_{ts}) stiffeners were varied from 2 to 4. Thus, in each plate arrangement configured, the influence of the ratio between the height of the transverse and longitudinal stiffeners (h_{ts}/h_{ls}) was analyzed, taking into account the values 0.50; 0.75; 1.00; 1.25; 1.50; 1.75 and 2.00, regarding to the maximum and central deflections. The results have shown that transforming a portion of steel from a non-stiffened reference plate into stiffeners can reduce the maximum and central deflections by more than 90%. Moreover, it was observed that to reduce the deflections it is more effective consider $h_{ts} > h_{ls}$, once the ratio $h_{ts}/h_{ls} = 2.00$ was the one that led to the better mechanical behavior among the analyzed cases.

1. Introduction

Plates are structural components whose the main characteristic is the thickness much less than the width and the length (Szilard, 2004). Due to this particularity the plates are susceptible to suffer out-of-plane displacements, being convenient to insert stiffeners with the purpose of increase its rigidity. Stiffened plates present a favorable relation between weight and load support, finding application in different engineering structures, such as ship hull (see Fig. 1), bridge deck and aircraft fuselage (Bedair, 2009; Ventsel & Krauthammer, 2001). Over the past decades, several researchers studied the mechanical behavior of stiffened plates using different approaches. O'Leary and Harari (1985) presented a model for stiffened plates analysis using Finite Element Method (FEM), where the restrictions between the plate and stiffeners were determined by Lagrangian multipliers. Kukreti and

* Corresponding author.
E-mail addresses: liercioisoldi@furg.br (L. A. Isoldi)

doi: 10.5267/j.esm.2020.12.001

Cheragni (1993), applying the principle of minimum potential energy presented a proposal for analysis of stiffened plates, so that the deflection in the plate was obtained by the product of polynomial and trigonometric series. Considering the system plate-stiffener rigidly connected, Bedair (1997) analyzed stiffened plates under bending applying Quadratic Sequential Programming, emphasizing the importance of investigate different geometric arrangements.

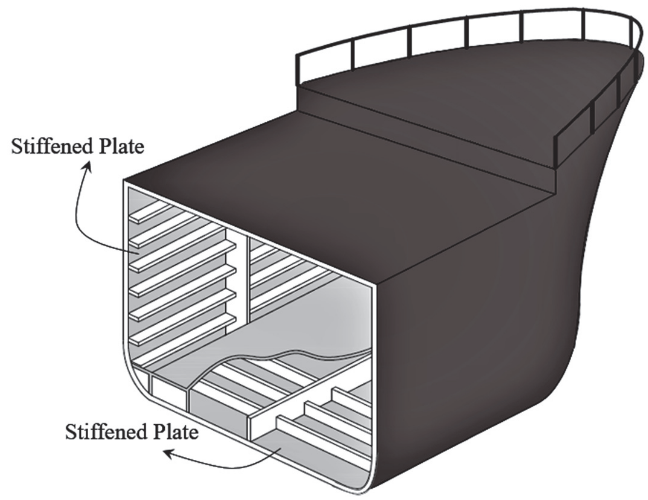

Fig. 1. Cross section of a ship

By employing genetic algorithms, Kallassy and Marcelin (1997) performed a topological optimization on stiffened plates. Guo et al. (2002) showed a semi-discrete finite element formulation to analyze stiffened plates and bridge decks composed by beam-slab system subject to transverse loading, considering the interaction between plate-stiffener in terms of bending deflections. As well, Khosravi et al. (2017) studied the mechanical behavior of composite steel plate shear walls subjected to transverse loading using the FEM through ABAQUS® software. Recently, studies dealing with the mechanical behavior of thin steel plates using Constructal Design Method (CDM) associated with FEM have shown interesting results. Isoldi et al. (2013a,b), Helbig et al. (2016a,b, 2018), and Da Silva et al. (2019) studied the buckling effect on perforated plates by the application of the CDM and FEM, as well, Lima et al. (2018, 2020) with respect to stiffened plates. Likewise, using the CDM and FEM, Cunha et al. (2018), De Queiroz et al. (2019), and Troina et al. (2020) carried out a geometric analysis on stiffened plates subjected to uniform transverse loading. It is worth to mention that in these studies about stiffened plates, the transverse and longitudinal stiffeners have always been considered with the same height. Therefore, the present study aimed to apply the CDM and the FEM in association to analyze several geometric arrangements of rectangular thin steel plates under uniform transverse loading, considering different quantities of longitudinal N_{ls} and transverse N_{ts} stiffeners and different ratios between the heights of the transverse h_{ts} and longitudinal h_{ls} stiffeners, seeking to minimize the maximum and central out-of-plane deflections. To do so, the analyzed stiffened plates were generated from a reference plate with no stiffeners and by means the ϕ volume fraction parameter (defined as the ratio between steel volume of the stiffeners and the total steel volume of the reference plate).

2. Computational Modeling

It is well known that the numerical methods are widely employed in the analysis of structures. With regard to stiffened plates, due to its geometric complexity the numerical simulation becomes a powerful approach, because allows obtaining an accurate solution since the analytical solutions for this kind of problem are practically nonexistent or have a complex mathematical solution (Szilard, 2004). The FEM consists in the discretization of a continuous domain in a set of elements with finite size, which are connected to each other by nodal points, converting the differential equation that governs the problem into algebraic equations solvable through a linear system (Burnett, 1987). According to

Zienkiewicz (1971), the FEM application in an elastic linear analysis consists of creating the model's geometry, generating the appropriate mesh, applying the loads and boundary conditions, and finally solving the problem. The numerical models adopted in this study were solved by the FEM through the ANSYS® Mechanical APDL software. The two-dimensional 8-node SHELL281 finite element in its quadrilateral version was employed, since it is suitable for modeling thin and moderately thick plates. The SHELL281 has 6 degrees of freedom per node: 3 rotations and 3 translations in relation to the *x*, *y* and *z* axes (ANSYS, 2019).

2.1. Computational Model Verification

The computational model verification was performed based on the case presented in Fig. 2, previously analyzed by Troina et al. (2018) through the FEM, using the three-dimensional element SOLID95 in the tetrahedral and hexahedral versions.

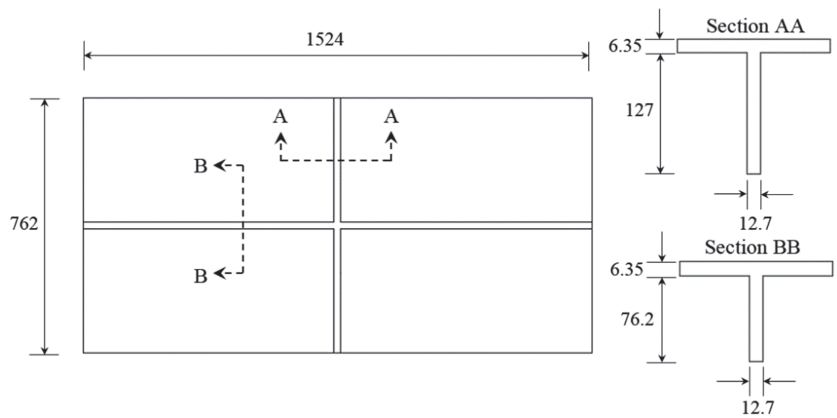

Fig. 2. Rectangular plate with two orthogonal stiffeners (unit: mm)

The stiffened plate of Fig. 2 is simply supported in its four edges being subjected to a uniform transverse loading of 68.95 kPa. It is made of steel with a Poisson's ratio of 0.30 and Young's modulus of 206.8427 GPa. So, this problem was solved employing the computational model developed with 8-node SHELL281 finite element, totaling 15,200 finite elements determined according to the convergence of results presented in Fig. 3. Still considering Fig. 3, it is possible to observe the results obtained by Troina et al. (2018).

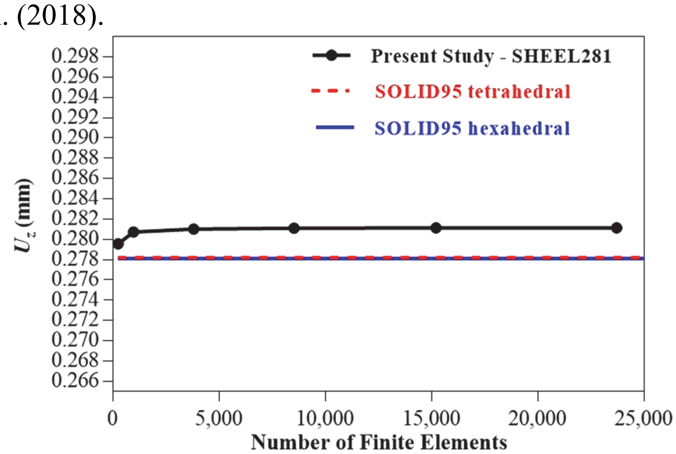

Fig. 3. Computational model verification.

From Fig. 3, it can be observed that the difference in central deflection U_z among the models with SHELL281 quadrilateral element and SOLID95 tetrahedral and hexahedral elements is about 1%. This difference can be explained due to the element SOLID95 considers all stress and strain components of the three-dimensional solid, while the two-dimensional element SHELL281 presents simplifications due to the stress and strain plane states. Therefore, the model developed in the present study can be considered as verified.

2.2. Computational Model Validation

For the numerical model validation, it was adopted the plate presented in the experimental study by Carrijo et al. (1999), as shown in Fig. 4. The square plate has eight stiffeners and as boundary conditions, just its four corners were considered simply supported. The plate was subjected to a uniform transverse load of 0.96 kPa and has an elastic modulus of 2.5 GPa and a Poisson's ratio of 0.36. The plate was solved using the SHELL281 element in its quadrangular version with a mesh of 2,436 finite elements, defined after the mesh convergence test presented in Fig. 5, which also shows the experimental result obtained in the study by Carrijo et al. (1999).

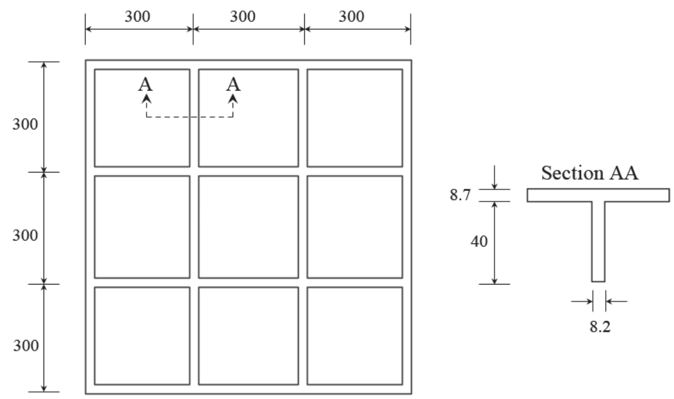

Fig. 4. Square plate with eight stiffeners (unit: mm).

By observing the Fig. 5, it is possible to notice that the numerical result for deflection in the center of the plate U_z = 6.505 mm, showed a difference of 4.58% in comparison with the value of U_z = 6.220 mm obtained in the experimental study, validating the computational model.

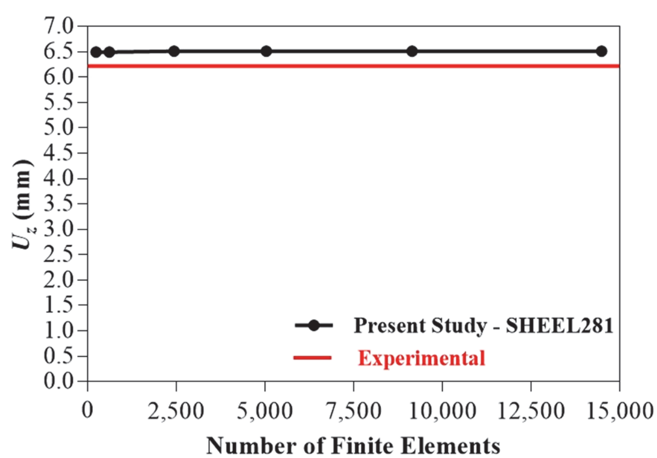

Fig. 5. Computational model validation.

3. Constructal Design Method (CDM)

According to Bejan & Zane (2012), the Constructal Law is a physical principle that governs the geometric shapes of the flow systems existing in nature. This law states that: “For a finite-size flow system to persist in time (to live), its configuration must evolve in order to facilitate access to the currents that flow through it”. The CDM is the application of the Constructal Law in physical problems, based on a principle of restrictions and objectives. The global performance of a system brings intrinsic restrictions, which may include the space destined for the development of the system, the available material and allowed rates of temperature, stress, strain, and pressure. Once the restrictions are determined, the degrees of freedom related to the geometric parameters are modified aiming to analyze their influence on a predefined performance indicator (Reis, 2006; Dos Santos et al., 2017).

It is important to mention that the CDM is widely employed in heat transfer and fluid mechanics engineering problems, being possible to find a lot of publications about this subject. However, the CDM application in structural engineering can be found only in some few publications, among which one can highlight the papers published by Bejan and Lorente (2008), Lorente et al. (2010), and Isoldi et al. (2013b). Based on the existing similarities among heat transfer, fluid mechanics and mechanics of materials, conceptually proved that CDM can also be used for structural engineering evaluations. On the other hand the application of CDM for buckling analysis of perforated steel plates (Rocha et al., 2013; Helbig et al., 2016a,b, 2018; Lorenzini et al., 2016; Da Silva et al., 2019), buckling analysis of stiffened steel plates (Lima et al., 2018,2020), and bending analysis of stiffened steel plates (Cunha et al., 2018; De Queiroz et al., 2019; Amaral et al., 2019; Pinto et al., 2019; Troina et al., 2020) can be seen in the literature. To apply the CDM in the present study, a non-stiffened steel plate with length a = 2000 mm, width b = 1000 mm and thickness t = 20 mm was taken as reference. From that, keeping constant a = 2000 mm, b = 1000 mm, and the total volume of material, a steel portion of reference plate was fully deducted from its thickness and transformed into stiffeners through ϕ parameter, which represents the ratio between the steel volume of stiffeners V_s and the steel volume of the reference plate V_r. The mathematical description of the ϕ parameter demanded different equations, owing to the consideration of different ratios between the heights of the transverse and longitudinal stiffeners h_{ts}/h_{ls}, Hence, for the case of $h_{ls} = h_{ts}$ it is defined:

$$\phi = \frac{V_s}{V_r} = \frac{N_{ls}(ah_{ls}t_s) + N_{ts}(bh_{ts}t_s) - N_{ls}N_{ts}\,t_s^2}{abt} \tag{1}$$

when $h_{ls} > h_{ts}$ is given by:

$$\phi = \frac{V_s}{V_r} = \frac{N_{ls}(ah_{ls}t_s) + N_{ts}(bh_{ts}t_s) - N_{ls}N_{ts}\,t_s^2 h_{ts}}{abt} \tag{2}$$

and finally for $h_{ls} < h_{ts}$:

$$\phi = \frac{V_s}{V_r} = \frac{N_{ls}(ah_{ls}t_s) + N_{ts}(bh_{ts}t_s) - N_{ls}N_{ts}\,t_s^2 h_{ls}}{abt} \tag{3}$$

where V_s is the material volume of the stiffeners and V_r is the material volume of the reference plate; h_{ls} and h_{ts} are the height of the stiffeners in the longitudinal and transverse directions, respectively. The length, width and thickness of the reference plate are a, b and t, respectively. Likewise, t_p represents the thickness of the stiffened plate. To identify the analyzed plate arrangements, the format P(N_{ls},N_{ts}) was adopted, being N_{ls} the number of longitudinal stiffeners and N_{ts} the number of transverse stiffeners. All aforementioned parameters are presented in Fig. 6, on a stiffened plate P(2,3).

Taking into consideration the results of Troina et al. (2020), it was adopted in this study the value of ϕ = 0.30, what means, 30% of the material from the reference plate transformed into stiffeners. A total of 27 stiffened plate arrangements were studied, varying the number of stiffeners from 2 to 4 in the longitudinal and transverse directions for 3 values of stiffeners thickness t_s (6.35 mm, 12.70 mm and 25.40 mm). In each of the arrangements, it was varied the ratio h_{ts}/h_{ls} considering the values 0.50; 0.75; 1.00; 1.25; 1.50; 1.75 and 2.00. So, for each new arrangement formed, the geometry influence caused on the maximum deflection $U_{zmáx}$ and central deflection U_z was registered, being these one the performance indicators which must be minimized. The Fig. 7 shows a flowchart including all the plate arrangements analyzed in this study.

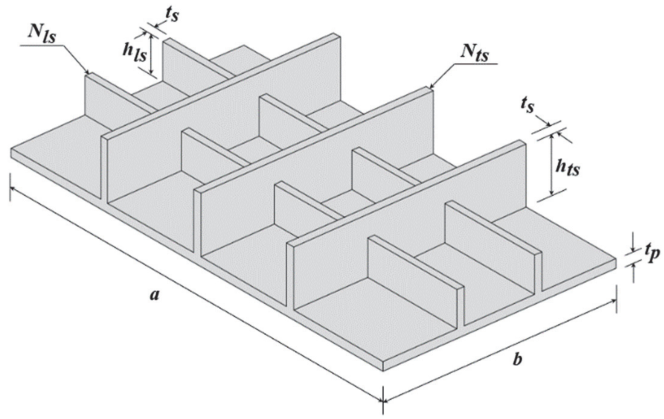

Fig. 6. Geometry and configuration of plate P(2,3).

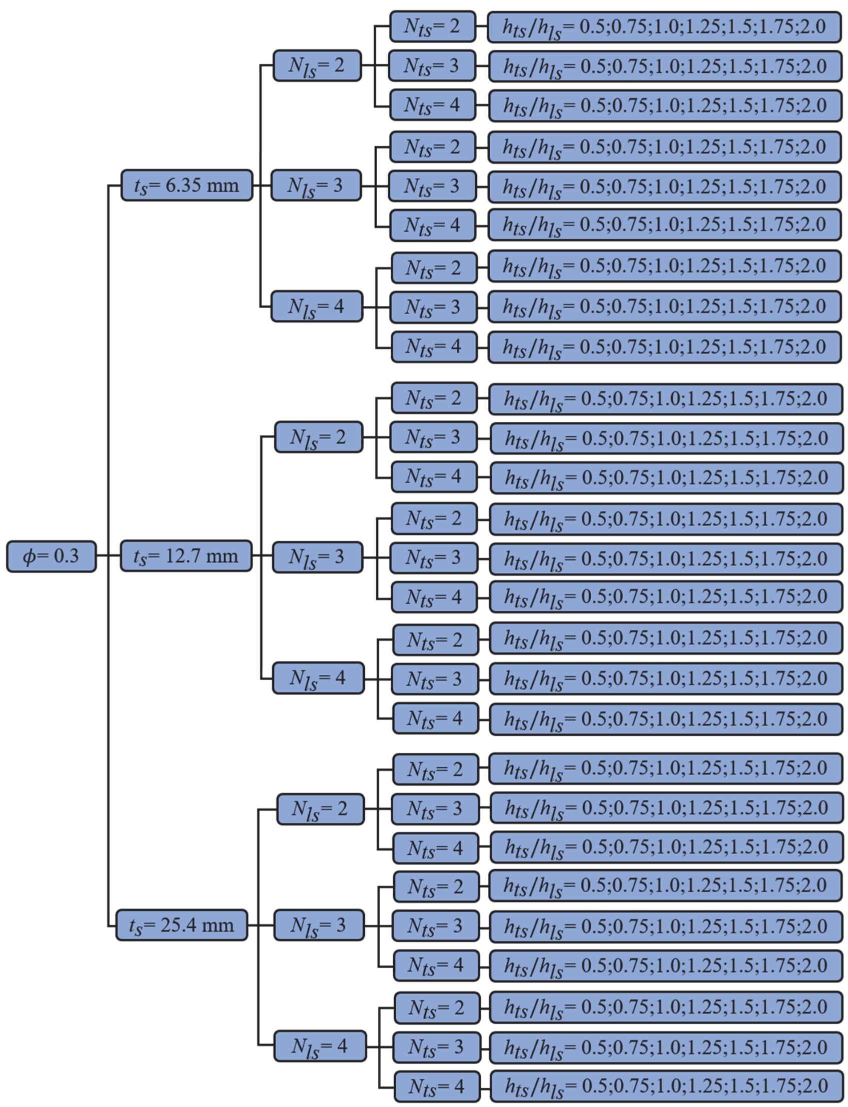

Fig. 7. Analyzed stiffened plate arrangements.

4. Results and Discussion

All the studied geometric configurations of plates (see Fig. 7), were subjected to a uniform transverse loading of 10 kPa with boundary conditions of simply supported edges. The material adopted was the A-36 steel with Poisson's ratio 0.30 and Young's modulus 200 GPa. A previous mesh convergence test was carried out in order to define the appropriate size of the finite elements used in the numerical simulations. To do so, the plate P(4,4) with stiffener thickness t_s = 6.35 mm and ratio h_{ts}/h_{ls} = 2.00 was adopted, since it presents the greatest number of stiffeners and the greatest difference between heights of longitudinal and transverse stiffeners among all the analyzed arrangements. The result of the mesh convergence test can be observed in Table 1.

Table 1. Mesh convergence test.

Mesh	Finite element size (mm)	U_{zMax} (mm)	U_z (mm)
1	300	0.01730	0.01810
2	200	0.01810	0.01810
3	100	0.01880	0.01880
4	50	0.01881	0.01881
5	25	0.01882	0.01882
6	12.5	0.01882	0.01882
7	6.25	0.01882	0.01882

According to the results presented in Table 1, it can be noted that from mesh number 5 composed by finite elements with 25 mm, there was a convergence of results for the maximum deflection U_{zMax} and central deflection U_z, so that it was the finite element size defined for spatial discretization of all studied stiffened plate arrangements. The results are exposed in Figs. 8, 9 and 10, showing for each plates arrangement, the values of U_{zMax} and U_z according to the variation of the degree of freedom h_{ts}/h_{ls}, taking account the 3 different stiffeners thicknesses considered (t_s = 6.35 mm, t_s = 12.70 mm, and t_s = 25.40 mm). Highlighting that, the Appendix "A" presents all these results in detail. Firstly, observing the Figs. 8, 9 and 10, as expected, it is possible to notice that transforming into stifenners a portion of material from the non-stiffened reference plate improves the mechanical behavior with regard to the maximum deflection U_{zMax} and central U_z, since all the results founded are less than the value of U_{zMax} = U_z = 0.697 mm obtained for the non-stiffened reference plate. Also it is possible to observe that for the 3 stiffeners thicknesses adopted, t_s = 6.35 mm, t_s = 12.70 mm, and t_s = 25.40 mm, the plates P(2,3) with ratio h_{ts}/h_{ls} = 2.00, were those which presented the lowest values of maximum and central deflections among all the arrangements considered in this study. Being the plate with t_s = 6.35 mm the one that showed the lowest maximum and central deflections among them.

Considering the plate P(2,3) with ratio h_{ts}/h_{ls} = 2.00 and t_s = 6.35 mm (see Fig. 8), it were obtained U_{zMax} = 0.0145 mm and U_z = 0.0083 mm, which means a reduction of 97.9% for maximum deflection and 98.8% for central deflection when compared with the reference plate. For plate P(2,3) with ratio h_{ts}/h_{ls} = 2.00 and t_s = 12.70 mm, were found the values of U_{zMax} = 0.0256 mm and U_z = 0.0189 mm, reaching in comparison to the reference plate a decrease of 96.3% for maximum deflection and 97.2% for central deflection. Regarding the plate P(2,3) with ratio h_{ts}/h_{ls} = 2.00 and t_s = 25.4 mm, the deflection values found were U_{zMax} = 0.0638 mm and U_z = 0.0559 mm, which represents a reduction of 90.8% for maximum deflection and 91.9% for central deflection compared to the reference plate. In its turn, establishing a comparison among the 3 better geometries, taking into account the plate P(2,3) with ratio h_{ts}/h_{ls} = 2.00 and t_s = 6.35 mm and comparing with the plate P(2,3) with ratio h_{ts}/h_{ls} = 2.00 and t_s = 12.70 mm, the plate with t_s = 6.35 mm showed values of maximum and central deflection 43.35% and 56.1% lower, respectively. Now, comparing the plate P(2,3) with ratio h_{ts}/h_{ls} = 2.00 and t_s = 6.35 mm with the plate P(2,3) with ratio h_{ts}/h_{ls} = 2.00 and t_s = 25.40 mm, the plate with t_s = 6.35 mm presented a reduction of 72.2% for maximum deflection and 85.1% for central deflection. The minimization of deflections presented by the three stiffened plates with better performance can be seen in Fig. 11.

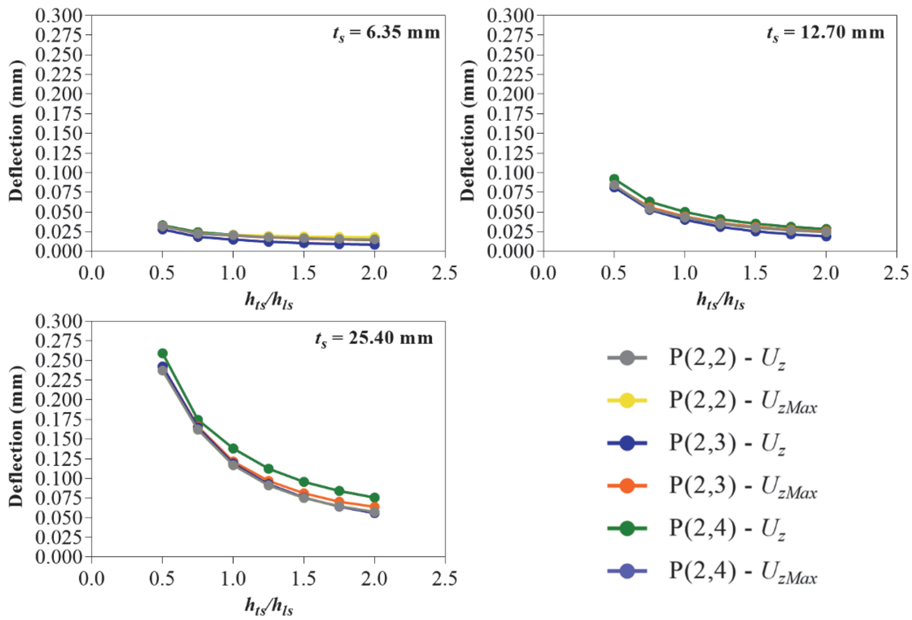

Fig. 8. Results for plates with N_{ls} = 2 and N_{ts} = 2, 3, 4.

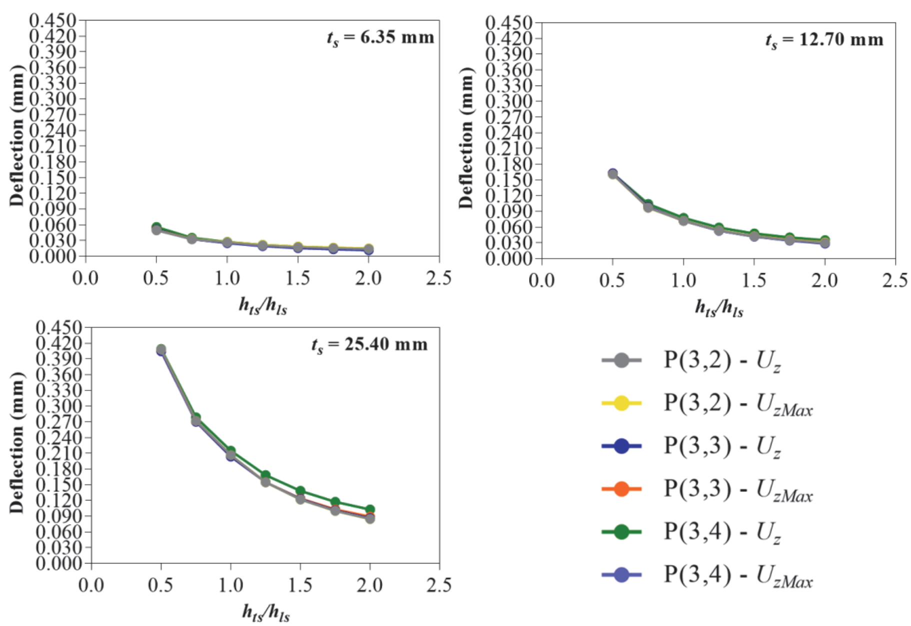

Fig. 9. Results for plates with N_{ls} = 3 and N_{ts} = 2, 3, 4.

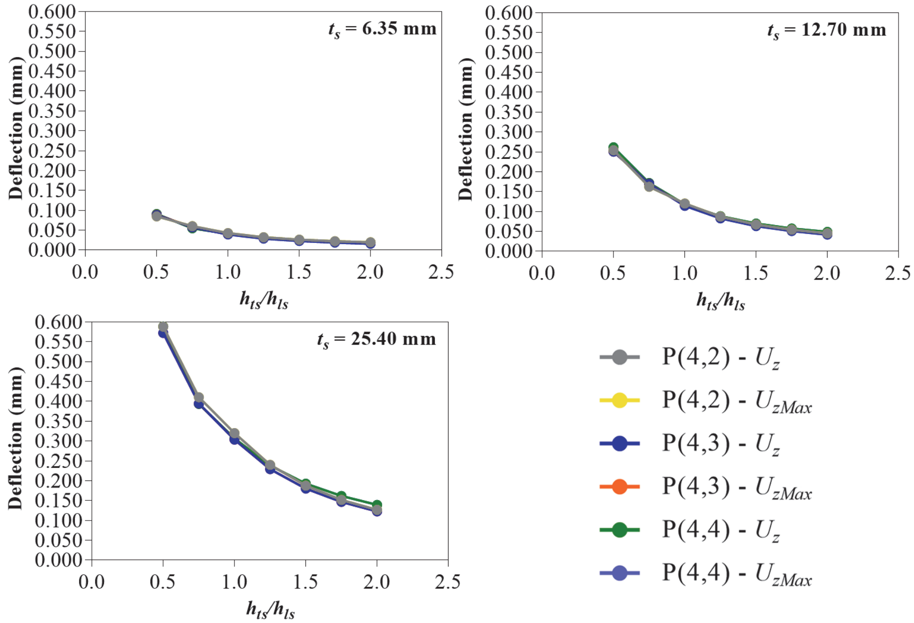

Fig. 10. Results for plates with N_{ls} = 4 and N_{ts} = 2, 3, 4.

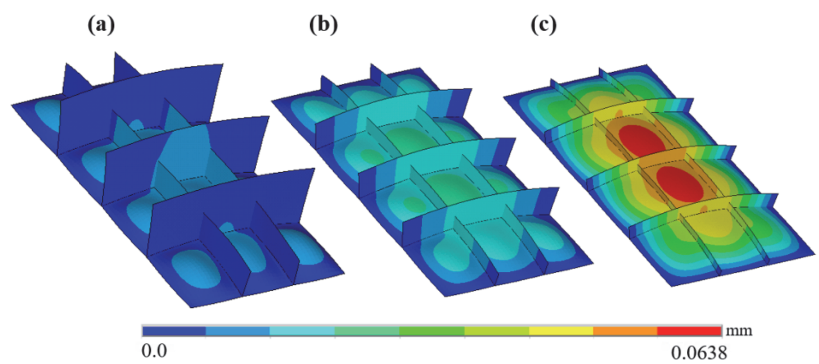

Fig. 11. Deflection distributions for P(2,3) with ratio h_{ts}/h_{ls} = 2.00: (a) t_s = 6.35 mm; (b) t_s =12.70 mm; (c) t_s = 25.40 mm

Based on the presented results, it is possible to observe the influence of the increase of the h_{ts}/h_{ls} ratio value on the mechanical behavior of the plates concerning of maximum and central deflections minimization, indicating that an increase in the height of the transverse stiffeners increases the stiffness of the stiffened plates, since the better results were for the ratio h_{ts}/h_{ls} = 2.00. According to Araújo (2014), this can be explained because the stiffened plate is rectangular, resulting in a greater inclination in the curvature of the bending moment diagram in the direction of the smaller span, i.e. in the transverse direction, which leads to greater bending moments, justifying the need to allocate a larger amount of steel in the transverse direction. It was also possible to infer that the maximum and central deflections were lower for the smaller adopted stiffener thickness (t_s = 6.35 mm). This occurred due to the fact that the material volume of the stiffeners is considered constant (30% of the material volume from reference plate), as well as the length and width of the plates as restrictions imposed according to the CDM. Thus, adopting a small stiffeners thickness, they become higher, increasing consequently the moment of inertia of the cross section, leading to greater rigidity of the plate. Still, considering the restrictions of the problem, it was observed that an increase in the number of stiffeners did not necessarily reduce the maximum and central deflections, since a greater quantity of stiffeners imply lower heights and consequently less moment of inertia. It is interesting to observe that in some cases the maximum and central deflection have not the same value. This is owing to the equidistant distribution of the stiffeners, such that when at least 1 stiffener crosses the center of the plate, it makes the region more rigid, shifting the deflection field to the less rigid regions (between the stiffeners), making different the maximum and central deflection. Otherwise, when none stiffener crosses the center of the plate, the region concentrates the highest deflections, so in these cases, the maximum and central deflection have the same value. Finally, as earlier mentioned, in the previous publications (for instance Cunha et al., 2018; De Queiroz et al., 2019; and Troina et al., 2020) only studies involving stiffened plates with h_{ts}/h_{ls} = 1.00 were carried out. Therefore, it is important here to identify the improvement obtained with the consideration of the h_{ts}/h_{ls} variation. If the best geometry among all analyzed cases (P(2,3) with ratio h_{ts}/h_{ls} = 2.00 and t_s = 6.35 mm) is compared with its corresponding geometry with h_{ts}/h_{ls} = 1.00 (i.e. P(2,3) with ratio h_{ts}/h_{ls} = 1.00 and t_s = 6.35 mm), one can affirm that it was achieved reductions of 27.50% and 43.92%, respectively, in maximum and central deflections of the stiffened plates; being this mechanical behavior improvement due solely to the steel redistribution among transverse and longitudinal stiffeners.

5. Conclusion

Through the application of the CDM in association with numerical models developed by means the FEM, it was possible to analyze different stiffened plates arrangements, showing the influence caused in the maximum and central deflections by varying the quantity and height of the longitudinal stiffeners h_{ls} and transverse h_{ts}.

First of all, as already inferred in previous works, it can be concluded that transform a material portion fully deduced from the thickness of an unstiffened plate into stiffeners, keeping the total volume of material constant, can improve the mechanical behavior reducting the maximum and central deflections by more than 90%. The results also showed that transverse stiffeners higher than longitudinal stiffeners are more effective in minimizing the maximum and central deflections, since the better results were for the ratio h_{ts}/h_{ls} = 2.00, i.e., when the transverse stiffeners were twice as high as the longitudinal. Besides, it was possible to conclude that for a constant volume of material, the increase in the number of stiffeners not generate lower maximum and central deflections. In addition, it is evident that associating the CDM with computational modeling through FEM can lead to great results with respect to mechanical behavior of stiffened plates, reaching a considerable improvement in the plate stiffness just modifying the geometric parameters. As suggestion for future researches, it is possible to investigate other thicknesses and quantities of stiffeners, even as other values for the volumetric fraction of stiffeners ϕ, concerning the minimization of deflections and/or stress.

Acknowledgement

This study was financed in part by the *Coordenação de Aperfeiçoamento de Pessoal de Nível Superior - Brasil* (CAPES) - Finance Code 001. The authors thank CAPES (Coordination of Superior Level Staff Improvement), FAPERGS (Foundation for Research Support of the State of Rio Grande do Sul), and CNPq (Brazilian National Council for Scientific and Technological Development). Particularly, the authors L. A. O. Rocha, E. D. dos Santos, and L. A. Isoldi thank CNPq for their research grants (Processes: 307791/2019-0, 306024/2017-9, and 306012/2017-0, respectively).

References

Amaral, R.R., Troina, G.S., Nogueira, C.M., Cunha, M.L., Rocha, L.A.O., Santos, E.D., & Isoldi, L.A. (2019). Computational modeling and constructal design method applied to the geometric evaluation of stiffened thin steel plates considering symmetry boundary condition. *Research on Engineering Structures and Materials*, 5, 393-402. DOI: 10.17515resm2019.112ms0204

ANSYS Academic Research Mechanical, Release 19, Help System, Element Reference, ANSYS, Inc.

Araújo, J.M. (2014). *Curso de concreto armado. 4 ed, vol.2.* Rio Grande: Dunas. (In Portuguese)

Bedair, O.K. (1997). Analysis of stiffened plates under lateral loading using sequential quadratic programming (SQP). *Computers & Structures*, 62(1), 63-80. DOI: 10.1016/S0045-7949(96)00281-7

Bedair, O. K. (2009). Analysis and Limit State Design of stiffened plates and shells: A world view. *Applied Mechanics Reviews*, 62(2), 01-16. DOI: 10.1115/1.3077137

Bejan, A. & Lorente, S. (2008). *Design with Constructal Theory*, Wiley: Hoboken, NJ, USA. DOI: 10.1002/9780470432709

Bejan, A. & Zane, J.P. (2012) *Design in Nature: How the Constructal Law governs evolution in biology, physics, technology, and social organizations.* New York: Doubleday.

Burnett, D. (1987). *Finite Element Analysis - From Concepts to Applications*. Massachusetts: Addison–Wesley.

Carrijo, E.C, Paiva, J.B. & Giogo, J.S. (1999). A numerical and experimental study of stiffened plates in bending. *Transactions on Modelling and Simulation*, 21, 12-18, DOI: 10.2495/CMEM990021

Cunha, M. L., Troina, G. S., Rocha, L. A. O., dos Santos, E. D. & Isoldi, L. A. (2018). Computational modeling and Constructal Design method applied to the geometric optimization of stiffened steel plates subjected to uniform transverse load. *Research on Engineering Structures and Materials*, 4(3), 139-149, DOI: 10.17515/resm2017.18st1118

Da Silva, C.C.C., Helbig, D., Cunha, M.L., Dos Santos, E.D., Rocha, L.A.O.; Real, M.V. & Isoldi, L.A. (2019). Numerical buckling analysis of thin steel plates with centered hexagonal perforation through constructal design method. *Journal of the Brazilian Society of Mechanical Sciences and Engineering*, 41(8), 309-1-309-18. DOI: 10.1007/s40430-019-1815-7

De Queiroz, J., Cunha, M.L., Pavlovic, A., Rocha, L. A. O, Dos Santos, E. D., Troina, G.S. & Isoldi, L.A. (2019). Geometric Evaluation of Stiffened Steel Plates Subjected to Transverse Loading for Naval and Offshore Applications. *Journal of Marine Science and Engineering*, 7(1), 7-18. DOI: 10.3390/jmse7010007

Dos Santos, E. D., Isoldi, L. A., Gomes, M. N., Rocha, L. A. O. (2017). *The Constructal Design Applied to Renewable Energy Systems*. In Rincón-Mejía. E & De las Heras. A (Eds.), Sustainable Energy Technologies 1ed. 63-87. Boca Raton: CRC Press - Taylor & Francis Group. DOI: 10.1201/9781315269979

Guo, M., Issam, E.H. & Ren, W. (2002). Semi-discrete finite element analysis of slab-girder bridges. *Computers & Structures*, 80(23), 1789-1796. DOI: 10.1016/S0045-7949(02)00207-9

Helbig, D., Da Silva, C.C.C., Real, M. V., Dos Santos, E.D., Isoldi, L.A. & Rocha, L.A.O. (2016a). Study About Buckling Phenomenon in Perforated Thin Steel Plates Employing Computational Modeling and Constructal Design Method. *Latin American Journal of Solids and Structures*, 13, 1912-1936. DOI: 10.1590/1679-78252893

Helbig, D., Real, M.V., Dos Santos, E.D., Isoldi, L.A. & Rocha, L.A.O. (2016b). Computational modeling and constructal design method applied to the mechanical behavior improvement of thin perforated steel plates subject to buckling. *Journal of Engineering Thermophysics*, 25, 197-215. DOI: 10.1134/S1810232816020053

Helbig, D., Cunha, M.L., Da Silva, C.C.C., Dos Santos, E.D., Iturrioz, I., Real, M.V., Isoldi, L.A. & Rocha, L.A.O. (2018). Numerical study of the elasto-plastic buckling in perforated thin steel plates using the constructal design method. *Research on Engineering Structures and Materials*, 4(3), 169-187. DOI: 10.17515/resm2017.37ds1123

Isoldi, L. A., Real, M.V., Vaz, J., Correia, A.L.G., Dos Santos, E. D. & Rocha, L. A. O. (2013a). Numerical analysis and geometric optimization of perforated thin plates subjected to tension or buckling. *Marine Systems & Ocean Technology*, 8(2), 99-107.

Isoldi, L. A., Real, M. V., Correia, A. L. G., Vaz, J., Dos Santos, E. D. & Rocha, L. A. O. (2013b). Flow of Stresses: Constructal Design of Perforated Plates Subjected to Tension or Buckling. In Rocha, L. A. O., Lorente, S., Bejan, A. (Ed.), *Constructal Law and the Unifying Principle of Design - Understanding Complex Systems 1ed*. (pp.195-127). New York: Springer.

Kallassy, A & Marcelin, J.L. (1997). Optimization of stiffened plates by genetic search. *Structural Optimization*, 13(1), 134-141.

Khosravi, H., Mousavi, S.S. & Tadayonfar, G. (2017). Numerical study of seismic behavior of Composite Steel Plate Shear Walls with flat and corrugated plates. *Revista de la construcción*, 16(2), 249-260.

Kurkaret, A.R & Cheragui, E. (1993). Analysis procedure for stiffened plate systems using an energy approach. *Computers & Structures*, 14(4), 649-657.

Lima, J.P.S., Rocha, L.A.O., Dos Santos, E.D., Real, M.V. & Isoldi, L.A. (2018). Constructal design and numerical modeling applied to stiffened steel plates submitted to elasto-plastic buckling. *Proceedings of the Romanian Academy Series A-Mathematics Physics Technical Sciences Information Science*, 19, 195-200.

Lima, J.P.S., Cunha, M.L., dos Santos, E. D. Rocha, L.A.O., Real, M.V. & Isoldi, L.A. (2020). Constructal Design for the ultimate buckling stress improvement of stiffened plates submitted to uniaxial compressive load. *Engineering Structures*, 203, 109883. DOI: 10.1016/j.engstruct.2019.109883

Lorente, S., Lee, J. & Bejan, A. (2010). The "flow of stresses" concept: the analogy between mechanical strength and heat convection. *International Journal of Heat and Mass Transfer*, 53, 2963–2968. DOI: 10.1016/j.ijheatmasstransfer.2010.03.038

Lorenzini, G., Helbig, D., Da Silva, C.C.C., Real, M.V., Dos Santos, E.D., Isoldi, L.A. & Rocha, L.A.O. (2016). Numerical Evaluation of the Effect of Type and Shape of Perforations on the Buckling of Thin Steel Plates by means of the Constructal Design Method. *International Journal of Heat and Technology*, 34, S9-S20. DOI: 10.18280/ijht.34S102

O'Leary, J. R. & Harari, I. (1985). Finite element analysis of stiffened plates. *Computers & Structures*, 21(5), 973-985.

Pinto, V.T., Cunha, M.L., Troina, G.S., Martins, K.L., dos Santos, E.D., Isoldi, L.A. & Rocha, L.A.O. (2019). Constructal design applied to geometrical evaluation of rectangular plates with inclined stiffeners subjected to uniform transverse load. *Research on Engineering Structures and Materials*, 5, 379-392. DOI: 10.17515resm2019.118ms0215

Reis, A.H. (2006). Constructal theory: from engineering to physics, and how flow systems develop shape and structure. *Applied Mechanics Reviews*, 59(5),269-281. DOI: 10.1115/1.2204075

Rocha, L.A.O., Isoldi, L.A., Real, M.V., Dos Santos, E.D., Correia, A.L.G., Biserni, C. & Lorenzini, G. (2013). Constructal design applied to the elastic buckling of thin plates with holes. *Central European Journal of Engineering*, 3, 475-483. DOI: 10.2478/s13531-013-0105-x

Szilard R. (2004). *Theories and applications of plate analysis: Classical numerical and engineering methods.* 1ª ed., Hoboken: Wiley. DOI: 10.1002/97804701728722

Troina, G.S.; de Queiroz, J.P.T.P., Cunha, M.L., Rocha, L.A.O., dos Santos E.D., & Isoldi, L.A. (2018). Verificação de modelos computacionais para placas com enrijecedores submetidas a carregamento transversal uniforme. CEREUS. v. 10, n. 2, p. 285-298. DOI: 10.18605/2175-7275/cereus.v10n2p285-298

Troina, G.S., Cunha, M.L., Pinto, V.T., Rocha, L.A.O., Dos Santos, E.D., Fragassa, C. & Isoldi, L.A. (2020). Computational Modeling and Design Constructal Theory Applied to the Geometric Optimization of Thin Steel Plates with Stiffeners Subjected to Uniform Transverse Load. *Metals*, 10, p. 1-29. DOI: 10.3390/met10020220

Ventsel, E. & Krauthammer, T. (2001). *Thin Plates and Shells: Theory, Analysis and Applications. 1ª ed*. New York: Marcel Dekker, Inc. DOI: 10.1201/9780203908723

Zienkiewicz, O.C. (1971). *The finite Element Method in Engineering Science*, *2º ed*. London: McGraw-Hill.

Appendix A

A.1. Results for plates with N_{ls} = 2 and N_{ts} = 2, 3, and 4.

	N_{ls}	N_{ts}	h_{ts} (mm)	h_{ls} (mm)	h_{ts}/h_{ls}	U_{zMax} (mm)	U_z (mm)
	2	2	189.458	378.915	0.50	0.0319	0.0319
	2	2	258.591	344.788	0.75	0.0223	0.0223
	2	2	316.300	316.300	1.00	0.0209	0.0203
t_s = 6.35 (mm)	2	2	364.842	291.873	1.25	0.0196	0.0180
	2	2	406.424	270.949	1.50	0.0189	0.0166
	2	2	442.443	252.825	1.75	0.0184	0.0157
	2	2	473.946	236.973	2.00	0.0181	0.0151

	N_{ls}	N_{ts}	h_{ts} (mm)	h_{ls} (mm)	h_{ts}/h_{ls}	U_{zMax} (mm)	U_z (mm)
	2	3	172.394	344.788	0.50	0.0319	0.0280
	2	3	227.813	303.751	0.75	0.0227	0.0183
	2	3	271.444	271.444	1.00	0.0200	0.0148
t_s = 6.35 (mm)	2	3	306.306	245.045	1.25	0.0176	0.0121
	2	3	334.989	223.326	1.50	0.0161	0.0104
	2	3	359.002	205.144	1.75	0.0152	0.0092
	2	3	379.398	189.699	2.00	0.0145	0.0083

	N_{ls}	N_{ts}	h_{ts} (mm)	h_{ls} (mm)	h_{ts}/h_{ls}	U_{zMax} (mm)	U_z (mm)
	2	4	158.150	316.30	0.50	0.0330	0.0330
	2	4	203.583	271.444	0.75	0.0244	0.0244
	2	4	237.730	237.730	1.00	0.0209	0.0209
t_s = 6.35 (mm)	2	4	263.957	211.166	1.25	0.0182	0.0182
	2	4	284.912	189.941	1.50	0.0164	0.0164
	2	4	302.039	172.594	1.75	0.0151	0.0151
	2	4	316.300	158.150	2.00	0.0142	0.0142

	N_{ls}	N_{ts}	h_{ts} (mm)	h_{ls} (mm)	h_{ts}/h_{ls}	U_{zMax} (mm)	U_z (mm)
	2	2	94.971	189.941	0.50	0.0843	0.0843
	2	2	129.746	172.995	0.75	0.0541	0.0541
	2	2	158.825	158.825	1.00	0.0432	0.0432
t_s = 12.70 (mm)	2	2	183.139	146.511	1.25	0.0350	0.0350
	2	2	203.955	135.970	1.50	0.0299	0.0299
	2	2	221.976	126.843	1.75	0.0267	0.0267
	2	2	237.730	118.865	2.00	0.0244	0.0244

	N_{ls}	N_{ts}	h_{ts} (mm)	h_{ls} (mm)	h_{ts}/h_{ls}	U_{zMax} (mm)	U_z (mm)
	2	3	86.498	172.995	0.50	0.0833	0.0814
	2	3	114.432	152.576	0.75	0.0560	0.0529
	2	3	136.469	136.469	1.00	0.0444	0.0401
t_s = 12.70 (mm)	2	3	153.914	123.131	1.25	0.0362	0.0311
	2	3	168.252	112.168	1.50	0.0312	0.0255
	2	3	180.246	102.998	1.75	0.0279	0.0216
	2	3	190.427	95.214	2.00	0.0256	0.0189

	N_{ls}	N_{ts}	h_{ts} (mm)	h_{ls} (mm)	h_{ts}/h_{ls}	U_{zMax} (mm)	U_z (mm)
	2	4	79.413	158.825	0.50	0.0922	0.0922
	2	4	102.352	136.469	0.75	0.0631	0.0631
	2	4	119.630	119.630	1.00	0.0502	0.0502
t_s = 12.70 (mm)	2	4	132.732	106.186	1.25	0.0410	0.0410
	2	4	143.187	95.458	1.50	0.0351	0.0351
	2	4	151.723	86.699	1.75	0.0311	0.0311
	2	4	158.825	79.413	2.00	0.0283	0.0283

	N_{ls}	N_{ts}	h_{ts} (mm)	h_{ls} (mm)	h_{ts}/h_{ls}	U_{zMax} (mm)	U_z (mm)
	2	2	47.729	95.458	0.50	0.2374	0.2374
	2	2	65.329	87.105	0.75	0.1620	0.1620
	2	2	80.096	80.096	1.00	0.1168	0.1168
t_s = 25.40 (mm)	2	2	92.297	73.837	1.25	0.0912	0.0912
	2	2	102.728	68.486	1.50	0.0752	0.0752
	2	2	111.750	63.857	1.75	0.0647	0.0647
	2	2	119.630	59.815	2.00	0.0574	0.0574

	N_{ls}	N_{ts}	h_{ts} (mm)	h_{ls} (mm)	h_{ts}/h_{ls}	U_{zMax} (mm)	U_z (mm)
	2	3	43.553	87.105	0.50	0.2426	0.2424
	2	3	57.749	76.999	0.75	0.1660	0.1648
	2	3	68.994	68.994	1.00	0.1216	0.1189
t_s = 25.40 (mm)	2	3	77.729	62.183	1.25	0.0968	0.0926
	2	3	84.894	56.596	1.50	0.0812	0.0757
	2	3	90.878	51.930	1.75	0.0704	0.0641
	2	3	95.950	47.975	2.00	0.0638	0.0559

	N_{ls}	N_{ts}	h_{ts} (mm)	h_{ls} (mm)	h_{ts}/h_{ls}	U_{zMax} (mm)	U_z (mm)
	2	4	40.048	80.096	0.50	0.2595	0.2595
	2	4	51.745	68.994	0.75	0.1745	0.1745
	2	4	60.594	60.594	1.00	0.1381	0.1381
t_s = 25.40 (mm)	2	4	67.133	53.706	1.25	0.1124	0.1124
	2	4	72.336	48.224	1.50	0.0956	0.0956
	2	4	76.576	43.757	1.75	0.0840	0.0840
	2	4	80.096	40.048	2.00	0.0757	0.0757

A.2. Results for plates with N_{ls} = 3 and N_{ts} = 2, 3, and 4.

	N_{ls}	N_{ts}	h_{ts} (mm)	h_{ls} (mm)	h_{ts}/h_{ls}	U_{zMax} (mm)	U_z (mm)
	3	2	135.351	270.703	0.50	0.0501	0.0498
	3	2	189.699	252.932	0.75	0.0334	0.0328
	3	2	237.351	237.351	1.00	0.0272	0.0264
t_s = 6.35 (mm)	3	2	279.158	223.326	1.25	0.0219	0.0209
	3	2	316.300	210.866	1.50	0.0187	0.0176
	3	2	349.516	199.723	1.75	0.0166	0.0154
	3	2	379.398	189.699	2.00	0.0152	0.0139

	N_{ls}	N_{ts}	h_{ts} (mm)	h_{ls} (mm)	h_{ts}/h_{ls}	U_{zMax} (mm)	U_z (mm)
t_s = 6.35 (mm)	3	3	126.466	252.932	0.50	0.0510	0.0510
	3	3	172.694	230.259	0.75	0.0329	0.0328
	3	3	211.316	211.316	1.00	0.0259	0.0252
	3	3	243.706	194.965	1.25	0.0208	0.0195
	3	3	271.444	180.962	1.50	0.0176	0.0160
	3	3	295.464	168.837	1.75	0.0156	0.0136
	3	3	316.468	158.234	2.00	0.0142	0.0119

	N_{ls}	N_{ts}	h_{ts} (mm)	h_{ls} (mm)	h_{ts}/h_{ls}	U_{zMax} (mm)	U_z (mm)
t_s = 6.35 (mm)	3	4	118.675	237.351	0.50	0.0560	0.0558
	3	4	158.487	211.316	0.75	0.0354	0.0350
	3	4	190.427	190.427	1.00	0.0277	0.0271
	3	4	216.244	172.995	1.25	0.0221	0.0214
	3	4	237.730	158.487	1.50	0.0187	0.0179
	3	4	255.891	146.224	1.75	0.0164	0.0155
	3	4	271.444	135.722	2.00	0.0148	0.0138

	N_{ls}	N_{ts}	h_{ts} (mm)	h_{ls} (mm)	h_{ts}/h_{ls}	U_{zMax} (mm)	U_z (mm)
t_s = 12.70 (mm)	3	2	67.861	135.722	0.50	0.1612	0.1612
	3	2	95.214	126.952	0.75	0.0974	0.0974
	3	2	119.246	119.246	1.00	0.0727	0.0726
	3	2	140.210	112.168	1.25	0.0542	0.0540
	3	2	158.825	105.883	1.50	0.0430	0.0426
	3	2	175.465	100.265	1.75	0.0358	0.0353
	3	2	190.427	95.214	2.00	0.0310	0.0303

	N_{ls}	N_{ts}	h_{ts} (mm)	h_{ls} (mm)	h_{ts}/h_{ls}	U_{zMax} (mm)	U_z (mm)
t_s = 12.70 (mm)	3	3	63.476	126.952	0.50	0.1629	0.1629
	3	3	86.800	115.734	0.75	0.0989	0.0989
	3	3	106.337	106.337	1.00	0.0723	0.0722
	3	3	122.576	98.061	1.25	0.0540	0.0536
	3	3	136.469	90.979	1.50	0.0430	0.0421
	3	3	148.490	84.852	1.75	0.0361	0.0345
	3	3	158.995	79.497	2.00	0.0315	0.0292

	N_{ls}	N_{ts}	h_{ts} (mm)	h_{ls} (mm)	h_{ts}/h_{ls}	U_{zMax} (mm)	U_z (mm)
t_s = 12.70 (mm)	3	4	59.623	119.246	0.50	0.1624	0.1624
	3	4	79.753	106.337	0.75	0.1043	0.1043
	3	4	95.950	95.950	1.00	0.0777	0.0777
	3	4	108.881	87.105	1.25	0.0595	0.0594
	3	4	119.630	79.753	1.50	0.0481	0.0480
	3	4	128.704	73.545	1.75	0.0406	0.0404
	3	4	136.469	68.234	2.00	0.0354	0.0351

	N_{ls}	N_{ts}	h_{ts} (mm)	h_{ls} (mm)	h_{ts}/h_{ls}	U_{zMax} (mm)	U_z (mm)
	3	2	34.117	68.234	0.50	0.4082	0.4082
	3	2	47.975	63.967	0.75	0.2722	0.2722
	3	2	60.202	60.202	1.00	0.2067	0.2067
t_s = 25.40 (mm)	3	2	70.745	56.596	1.25	0.1549	0.1549
	3	2	80.096	53.398	1.50	0.1220	0.1220
	3	2	88.447	50.541	1.75	0.1002	0.1002
	3	2	95.950	47.975	2.00	0.0851	0.0850

	N_{ls}	N_{ts}	h_{ts} (mm)	h_{ls} (mm)	h_{ts}/h_{ls}	U_{zMax} (mm)	U_z (mm)
	3	3	31.983	63.967	0.50	0.4050	0.4050
	3	3	43.861	58.481	0.75	0.2706	0.2706
	3	3	53.862	53.862	1.00	0.2041	0.2041
t_s = 25.40 (mm)	3	3	62.024	49.619	1.25	0.1551	0.1549
	3	3	68.994	45.996	1.50	0.1240	0.1231
	3	3	75.015	42.866	1.75	0.1035	0.1016
	3	3	80.269	40.135	2.00	0.0893	0.0863

	N_{ls}	N_{ts}	h_{ts} (mm)	h_{ls} (mm)	h_{ts}/h_{ls}	U_{zMax} (mm)	U_z (mm)
	3	4	30.101	60.202	0.50	0.4093	0.4093
	3	4	40.396	53.862	0.75	0.2789	0.2789
	3	4	48.729	48.729	1.00	0.2149	0.2149
t_s = 25.40 (mm)	3	4	55.216	44.173	1.25	0.1686	0.1686
	3	4	60.594	40.396	1.50	0.1384	0.1384
	3	4	65.125	37.214	1.75	0.1177	0.1177
	3	4	68.994	34.497	2.00	0.1029	0.1029

A.3. Results for plates with N_{ls} = 4 and N_{ts} = 2, 3, and 4.

	N_{ls}	N_{ts}	h_{ts} (mm)	h_{ls} (mm)	h_{ts}/h_{ls}	U_{zMax} (mm)	U_z (mm)
	4	2	105.284	210.568	0.50	0.0850	0.0850
	4	2	149.793	199.723	0.75	0.0604	0.0604
	4	2	189.941	189.941	1.00	0.0425	0.0425
t_s = 6.35 (mm)	4	2	226.066	180.852	1.25	0.0324	0.0324
	4	2	258.891	172.594	1.50	0.0262	0.0262
	4	2	288.849	165.056	1.75	0.0222	0.0222
	4	2	316.300	158.150	2.00	0.0195	0.0195

	N_{ls}	N_{ts}	h_{ts} (mm)	h_{ls} (mm)	h_{ts}/h_{ls}	U_{zMax} (mm)	U_z (mm)
	4	3	99.862	199.723	0.50	0.0885	0.0885
	4	3	139.051	185.401	0.75	0.0576	0.0572
	4	3	172.995	172.995	1.00	0.0399	0.0391
t_s = 6.35 (mm)	4	3	202.351	161.881	1.25	0.0302	0.0290
	4	3	228.163	152.108	1.50	0.0243	0.0228
	4	3	251.035	143.449	1.75	0.0206	0.0188
	4	3	271.444	135.722	2.00	0.0180	0.0160

	N_{ls}	N_{ts}	h_{ts} (mm)	h_{ls} (mm)	h_{ts}/h_{ls}	U_{zMax} (mm)	U_z (mm)
	4	4	94.971	189.941	0.50	0.0906	0.0906
	4	4	129.746	172.995	0.75	0.0550	0.0550
	4	4	158.825	158.825	1.00	0.0413	0.0413
t_s = 6.35 (mm)	4	4	183.139	146.511	1.25	0.0315	0.0315
	4	4	203.955	135.97	1.50	0.0255	0.0255
	4	4	221.976	126.843	1.75	0.0216	0.0216
	4	4	237.730	118.865	2.00	0.0188	0.0188

	N_{ls}	N_{ts}	h_{ts} (mm)	h_{ls} (mm)	h_{ts}/h_{ls}	U_{zMax} (mm)	U_z (mm)
	4	2	52.791	105.583	0.50	0.2542	0.2542
	4	2	75.199	100.265	0.75	0.1625	0.1625
	4	2	95.458	95.458	1.00	0.1202	0.1202
t_s = 12.70 (mm)	4	2	113.585	90.868	1.25	0.0873	0.0873
	4	2	130.049	86.699	1.50	0.0671	0.0671
	4	2	145.068	82.896	1.75	0.0541	0.0541
	4	2	158.825	79.413	2.00	0.0453	0.0453

	N_{ls}	N_{ts}	h_{ts} (mm)	h_{ls} (mm)	h_{ts}/h_{ls}	U_{zMax} (mm)	U_z (mm)
	4	3	50.133	100.265	0.50	0.2508	0.2508
	4	3	69.917	93.223	0.75	0.1696	0.1696
	4	3	87.105	87.105	1.00	0.1145	0.1143
t_s = 12.70 (mm)	4	3	101.840	81.472	1.25	0.0835	0.0827
	4	3	114.785	76.524	1.50	0.0646	0.0633
	4	3	126.248	72.142	1.75	0.0525	0.0506
	4	3	136.469	68.234	2.00	0.0444	0.0418

	N_{ls}	N_{ts}	h_{ts} (mm)	h_{ls} (mm)	h_{ts}/h_{ls}	U_{zMax} (mm)	U_z (mm)
	4	4	47.729	95.458	0.50	0.2619	0.2619
	4	4	65.329	87.105	0.75	0.1717	0.1717
	4	4	80.096	80.096	1.00	0.1184	0.1184
t_s = 12.70 (mm)	4	4	92.297	73.837	1.25	0.0883	0.0883
	4	4	102.728	68.486	1.50	0.0695	0.0695
	4	4	111.750	63.857	1.75	0.0572	0.0572
	4	4	119.630	59.815	2.00	0.0487	0.0487

	N_{ls}	N_{ts}	h_{ts} (mm)	h_{ls} (mm)	h_{ts}/h_{ls}	U_{zMax} (mm)	U_z (mm)
	4	2	26.546	53.093	0.50	0.5889	0.5889
	4	2	37.906	50.541	0.75	0.4110	0.4110
	4	2	48.224	48.224	1.00	0.3204	0.3204
t_s = 25.40 (mm)	4	2	57.353	45.882	1.25	0.2405	0.2405
	4	2	65.636	43.757	1.50	0.1877	0.1877
	4	2	73.186	41.821	1.75	0.1520	0.1520
	4	2	80.096	40.048	2.00	0.1270	0.1270

	N_{ls}	N_{ts}	h_{ts} (mm)	h_{ls} (mm)	h_{ts}/h_{ls}	U_{zMax} (mm)	U_z (mm)
t_s = 25.40 (mm)	4	3	25.271	50.541	0.50	0.5729	0.5729
	4	3	35.357	47.143	0.75	0.3948	0.3948
	4	3	44.173	44.173	1.00	0.3036	0.3036
	4	3	51.598	41.279	1.25	0.2296	0.2294
	4	3	58.110	38.740	1.50	0.1813	0.1803
	4	3	63.867	36.495	1.75	0.1488	0.1467
	4	3	68.994	34.497	2.00	0.1261	0.1228

	N_{ls}	N_{ts}	h_{ts} (mm)	h_{ls} (mm)	h_{ts}/h_{ls}	U_{zMax} (mm)	U_z (mm)
t_s = 25.40 (mm)	4	4	24.112	48.224	0.50	0.5892	0.5892
	4	4	33.130	44.173	0.75	0.3940	0.3940
	4	4	40.750	40.750	1.00	0.3065	0.3065
	4	4	46.893	37.514	1.25	0.2382	0.2382
	4	4	52.132	34.755	1.50	0.1929	0.1929
	4	4	56.653	32.373	1.75	0.1616	0.1616
	4	4	60.594	30.297	2.00	0.1391	0.1391